Current Research in Food Science 9 (2024) 100903

Contents lists available at ScienceDirect

Current Research in Food Science

journal homepage: www.sciencedirect.com/journal/current-research-in-food-science

Acetate cellulose fibrous scaffold is suitable for cultivated fat production

Amanda Maria Siqueira Moreira [a], Júlia Meireles Nogueira [a], Jade Carceroni [a], Jorge Luís Guadalupe [a], Ana Elisa Antunes dos Santos [a], Ana Maria Alvarenga Fagundes [a], Aline Gonçalves Lio Copola [a], Gerluza Aparecida Borges Silva [a], Aline Bruna da Silva [b], João Paulo Ferreira Santos [b], Juliano Douglas Silva Albergaria [b], Luciana de Oliveira Andrade [a], Erika Cristina Jorge [a,*]

[a] Department of Morphology, Institute of Biological Science, Federal University of Minas Gerais, Belo Horizonte, Brazil
[b] Laboratory of Biomaterials, Department of Materials Engineering, Federal Center for Technological Education of Minas Gerais (CEFET-MG), Belo Horizonte, Brazil

ARTICLE INFO

Handling Editor: Professor A.G. Marangoni

Keywords:
Adipocytes
Adipogenic differentiation
Cellulose acetate
Cultivated fat
Electrospinning
Scaffold

ABSTRACT

Fat is an essential component of meat which contributes to its sensory characteristics. Therefore, producing cultivated fat is essential to replicate the texture, flavor, and juiciness of conventional meat. One of the challenges in obtaining cultivated fat is that once adipocytes reach differentiation in culture, they tend to float. In this study, we tested whether immortalized pre-adipocytes could be viable, grow, and differentiate when cultivated onto a fibrous scaffold produced by the electrospun of cellulose acetate. Our results demonstrated that the cells attach, proliferate, colonize, and differentiate into mature adipocytes in the three-dimensional fibrous structure during the culture period. Moreover, when layers of the scaffold containing differentiated cells were stacked, it acquired a characteristic similar to conventional animal fat. Therefore, this research suggests that fibrous scaffolds produced using cellulose acetate are a promising substrate for producing cultivated fat.

1. Introduction

Cultivated meat is an edible biomass produced by *in-vitro* culture of stem cells harvested from live animals(Kumar et al., 2021). It is based on advances in stem cell biology and tissue engineering, initially developed for medical applications (Rubio et al., 2020). This technology presents as an alternative and a complement to animal agriculture production, reducing the need for livestock and all the issues it faces (Seah et al., 2022).

Most of the studies on cultivated meat have focused on mimicking the muscle tissue due to this component being the majority in traditional meat products (Zagury et al., 2022). However, even in a smaller fraction, adipose tissue plays an important role in sensory quality traits of meat, as texture and flavor(Hocquette et al., 2010). In fact, the latter is one of the challenges of plant-based meats and fats, once they do not provide the same sensory experience of the animal product (Yuen et al., 2022)

Animal intramuscular fat is composed of white adipose tissue, which main cell type is the adipocyte (Sugii et al., 2023). As for muscles, adipose tissue can be also reproduced in vitro. Preadipocytes are the most used cells to produce cultivated fat as they are adipose progenitor cells that are committed to adipogenesis (differentiation into mature adipocytes), while still being capable of proliferation (Yuen et al., 2022; Cawthorn et al., 2012). However, one of the main challenges in cultivating adipocytes is that during adipogenesis process, as lipid accumulation increases and cells become buoyant, they detach from the bottom of the plastic, and float to the surface of culture systems (Yuen et al., 2022; Louis and Matsusaki, 2020).

One alternative to avoid cellular fluctuation is the cultivation of these cells onto scaffolds. Scaffolds are biomaterials that mimic the extracellular matrix so that cells can attach, proliferate and/or differentiate. Several scaffolding technologies have been proposed to fabricate 3D structures with suitable biological, structural, and mechanical characteristics (Levi et al., 2022). For tissue maturation purposes, scaffolds can be categorized as porous scaffolds, hydrogels, or fiber scaffolds (Bomkamp et al., 2022).

For cultivated fat, most studies have focused on using hydrogels as scaffolds because they allow for cell immobilization in a 3D matrix and prevent flotation (Fish et al., 2020). For example, Dohmen et al. (2022) produced bovine adipose tissue using alginate hydrogels, while Liu et al. (2023) produced porcine adipose tissue using collagen hydrogels.

* Corresponding author.
E-mail addresses: erika.cris.jorge@gmail.com, ecjorge@icb.ufmg.br (E.C. Jorge).

https://doi.org/10.1016/j.crfs.2024.100903
Received 28 August 2024; Received in revised form 21 October 2024; Accepted 27 October 2024
Available online 28 October 2024

Alternatively, some studies have used porous scaffolds made of peanut protein (Song et al., 2022a), or rye secalin (Su et al., 2024), to produce cultivated pork fat.

The use of fibrous-type scaffolds for this purpose has not been reported thus far. Fibrous scaffolds are obtained through spinning techniques, producing nanofibers with a variety of properties useful for cultured meat (Bomkamp et al., 2022). This nanofiber scaffolds have gained much attention as a promising material for soft tissue engineering applications due to their structural similarity to mimic the architecture of the extracellular matrix (Unnithan et al., 2018).

Using electrospinning technology, our research group has developed a nanofibrous scaffold made of cellulose acetate (CAN), which has shown to be interesting for cultivated meat applications, due to its low-cost and relatively easy fabrication(Santos et al., 2023a). These cellulose acetate nanofiber showed high biocompatibility and efficient rates of adhesion, proliferation and differentiation of skeletal muscle cells (Santos et al., 2023a, 2023b). Using CAN we were able to produce structured cultivated meat by stacking several layers of CAN sheets containing differentiated skeletal muscle cells.

In the present work, we tested whether CAN would be also suitable for cultivated fat production. For this, we used a cell line model of adipogenesis, known as 3T3-L1, seeded onto CAN and evaluated its potential to allow cell attachment, growth and differentiation. Our results showed that CAN was able to prevent cellular flotation, while maintaining both cell proliferation and differentiation. This suggests that CAN could be used for cultivated fat production and for stacking with muscle tissue layers to produce a meat product.

2. Methodology

2.1. Scaffolds preparation

Cellulose acetate nanofibers (CAN) were obtained by electrospinning as described in Santos et al. (dos Santos et al., 2021). In brief, cellulose acetate in powder form with Mn ~30,000 g/mol, density of 1.3 g/mL, and 40% degree of substitution (Sigma-Adrich) was dissolved in acetone-dimethylformamide (DMF, 3:1 v/v, Labsynth) to obtain a 12% (w/v) solution. It was obtained a film formed by nanofibers randomly oriented with rotation at 400 rpm, voltage 16 kV, collecting distance 14 cm and solution gravity-fed at room temperature. The nanofibrous membranes were dried in a vacuum chamber for 3 days to remove the remaining solvents.

Before cell seeding, the CAN were cut into 16 mm diameter discs using laser cutting machine from IdeiaReal Bio Lab (UFMG, Belo Horizonte, Brazil) and sterilized using gamma irradiation (10 kGy) at Laboratório de Irradiação Gamma, installed at the Centro de Desenvolvimento da Tecnologia Nuclear (CDTN, Belo Horizonte, Brazil). Before cell seeding, CAN scaffolds were hydrated using growth medium for 30 min.

2.2. 3T3-L1 cell culture

3T3-L1 pre-adipocytes were maintained in growth medium (GM: DMEM supplemented with 10% FBS and 1% anti-anti), under 37 °C and 5% CO2 atmosphere. Cells were seeded at a density of 1×10^5 cells/well in a 24-well plate onto CAN or as monolayer at a density of 1×10^4 cells/well, to be used as control. To induce cell differentiation, after 3 days the GM was replaced by the adipogenic induction medium (IM: DMEM supplemented with 10% FBS, 1% anti-anti, 10 μg/ml insulin, 1 μM dexamethasone, 0.5 mM 3-isobutyl-1-methylxanthine and 0.1 mM indomethacin). After 2 days in IM, the medium was replaced with maintenance medium (MM: DMEM supplemented with 10% FBS, 1% anti-anti, and 10 μg/ml insulin) and kept under 37 °C and 5% CO2 atmosphere for up to 10 days. The medium was changed every 2 days during this period.

2.3. Cell viability and proliferation

Cell viability was evaluated using both the Live/Dead staining and MTT (3–94,5-dimethylthiazol-2-yl)-2,5-diphenyl tetrazolium bromide) assays (both Invitrogen). For Live/Dead, 3T3-L1 cells were seeded onto CAN in GM. After 24 and 72 h, cells were stained with 2 μM calcein-AM and 4 μM ethidium homodimer-1 in PBS at 37 °C for 30 min at room temperature (RT), followed by rinsing in PBS. Cell staining was evaluated using a fluorescence microscope (Olympus microscope BX50) under the excitation wavelengths of 490 and 528 nm (green = live cells; red = dead cells). For MTT assay, after 24, 48 and 72 h of cell seeding, the GM was replaced with the MTT solution and the samples incubated for 4 h at 37 °C and 5% CO2. Formazan crystals were then dissolved in 1 ml/well in isopropanol-acid. After that, the solution was transferred to a 96-well plate in triplicate and absorbance were measured at 595 nm using a microplate reader (Elx800-Biotek).

2.4. Lipid droplets staining

Lipid droplets accumulation were detected using BODIPY (Invitrogen) and Oil red O (Sigma-Aldrich) staining. For both, 3T3-L1 cells were cultivated to induce adipogenic differentiation onto CAN or as monolayer. Both analyzes were performed after 4, 7, 10, 12 and 15 days of culture. For the Bodipy staining, cells were rinsed in PBS and then incubated at 37 °C for 15 min with 200 μl of the BODIPY-culture media solution per well. Cells were then fixed in 4% PFA for 15 min at RT and the nuclei were counterstained using DAPI (Invitrogen) for 3 min and maintained in mounting media. Images were obtained in either an Olympus fluorescence microscope BX50 or using the confocal microscope Zeiss LSM 880 (from CAPI-ICB-UFMG). This last method also enabled the acquisition of images at various focal planes throughout the sample's depth, allowing observation of cell infiltration along the Z-axis.

For the Oil red O staining, cells were washed with PBS, fixed with 4% PFA at RT for 15 min and then washed with PBS. Cells were then incubated with Oil red O for 30 min at RT and washed 3 times in PBS. Staining was documented using the bright field of the Motic AE31 inverted microscope. Lipid droplets were quantified in triplicate. For this, Oil red O staining was dissolved in 1 ml of isopropanol for 10 min and transferred to a 96-well plate in triplicate. Absorbance was measured at 490 nm using the microplate reader (Elx800-Biotek).

2.5. Scanning electron microscopy (SEM)

For SEM analysis, 3T3-L1 cells were cultivated to induce adipogenic differentiation onto the CAN only. After 1, 2, 3, 5, 7, 10, 12 and 15 days of culture, cells were fixed with 2.5% glutaraldehyde in 0.1M phosphate buffer for 2 h at RT. Cells were then rinsed in PBS, dehydrated in a graded series of ethanol baths (35, 50, 70, 85, 95 and 100% for 15 min/bath). Samples were dried at critical point and gold coated. Images were obtained using Quanta 200 FEG SEM (FEI, Hillsboro, USA).

2.6. Gene expression by qPCR

For gene expression analysis, 3T3-L1 cells were cultivated to induce adipogenic differentiation onto the CAN or as monolayer. After 1, 3, 5, 10 and 15 days of culture, total RNA was isolated using TRI-Reagent (Sigma-Aldrich), according to the manufacturer's instructions, and 1 μg was reverse transcribed in cDNA following the instructions in the RevertAid H minus first strand cDNA synthesis kit (Thermo Fischer Scientific). qPCR was performed using 0.4–0.8 μM of each primer, 1 μl (diluted 1:10) of each cDNA, and 5 μl of iTaq Universal SYBR Green Supermix (Bio-Rad), and nuclease-free water to final volume of 10 μl. The reactions were performed in the Real-Time PCR Cycler Rotor Gene 3000 Machine (Corbett Research), using the following cycle parameter: 50 °C for 2 min, 95 °C for 2 min, followed by 45 cycles of 94 °C for 15 sec, 60–62 °C for 15 sec, and 72 °C for 20 sec. The dissociation step was

performed at the end of the amplification step to allow identifying specific melting temperature for each initiator set. Relative quantification was performed in triplicate, using *GAPDH* as reference gene. The sequences of forward and reverse primers were as follows: *GAPDH* (AGGTCGGTGTGAACGGATTTG and TGTAGACCATGTAGTTGAGG TCA); *C/EBPβ* (GAAGACGGTGGACAAGCTGA and TGCTCCACCT TCTTCTGCAG); *PPARγ* (ATTGAGTGCCGAGTCTGTGG and GGCATTGT GAGACATCCCCA); and *Plin1* (GCCAAACCAAGCCTTGTGAG and GTCGTCTGTCTCCTCTCCCT).

2.7. Stacking

In order to obtain a thick fat structure, four layers of 3T3-L1 cells cultivated in adipogenic differentiation medium for 12 days were overlaid on each other for stacking and maintained for an additional 3 days in MM. To assessing the heat stability and observe whether the visual characteristics of the cultured adipose tissue resembled those of conventional adipose tissue during the cooking process, the stacked structure was subjected to a frying process. For this, the culture medium was removed, and the sample was washed with PBS. It was then placed in a preheated Teflon pan at 200 °C and baked until it reached a golden color.

2.8. Statistical analysis

All quantitative analyses were conducted in triplicate and carried out using GraphPad Prism (version 8.0, San Diego, CA, USA). The data related to the analyses of MTT, Oil red O, and Z-stack confocal are presented as means ± SD (standard deviations). Gene expression analysis was conducted using REST software (Pfaffl et al., 2002), employing a pairwise fixed reallocation randomization test and taking into account primer efficiency. The data are presented as means ± SEM (standard error of the mean).

3. Results

In this work, we tested whether cellulose acetate nanofibers could be used as scaffolds to allow the attachment, growth and differentiation of 3T3-L1 pre-adipocytes into mature adipocytes, capable of producing lipid droplets when attached to a substrate to avoid cell floating.

3.1. 3T3-L1 cell viability and proliferation onto the CAN

We first investigated whether 3T3-L1 cells were viable and could proliferate when cultivated onto the CAN. Cell viability was assessed only during the growth stage (culture in GM), after 1 and 3 days of culture using Live and Dead assay and 1, 2 and 3 days using MTT assay.

Live and Dead analysis revealed that the majority of the cells were viable when cultivated onto CAN for 1 (Fig. 1A–C) and 3 (Fig. 1D–F) days and only few cells were found dead (Fig. 1B and E). MTT analysis revealed no difference in the cell viability index of the cells between 1 and 2 days of culture, while a significant increase in the index was observed after 3 days of culture in GM (Fig. 1G).

The lack of significant differences in viability during the early days of culture is promising, and the notable increase in the index after three days suggests that the CAN is non-cytotoxic.

3.2. CAN colonization by 3T3-L1 cells during culture

In order to determine whether 3T3-L1 cells could colonize the surface and also penetrate into the CAN porous structure, we evaluated the surface morphology using SEM (Fig. 2A–D, G, J and M) and the DAPI + Bodipy staining through the CAN thickness using the Z-stack analysis of confocal images (Fig. 2B–E, H, K and N) after 1, 3, 7, 10 and 15 days of culture.

Our results revealed that the cells could colonize and infiltrate the CAN structure from day 1 of culture, as SEM images allowed the observation of cells under the cellulose acetate fibers (Fig. 2A, arrowheads). An increasing number of cells growing inside the CAN mesh could be observed after 3 days (Fig. 2D). From 7 days of culture, we could observe the appearance of round shaped cells, together with flat cells, colonizing the CAN (Fig. 2G–J and M).

Fluorescence images from the DAPI + Bodipy staining captured along the z-axis using confocal microscopy allowed the three-dimensional analysis of the infiltration of the cells into the CAN. Bodipy was also able to label CAN, which helped determine cell infiltration along the nanofiber. Cell infiltration, as seen in SEM images, could be observed from the first day of culture (Fig. 2C). By day 15, cells apparently had reached the other side of the CAN (Fig. 2O). The infiltration rate revealed that the cells reached a depth of 37 μm on the first day of culture (Fig. 2P), and during cultivation, penetration gradually increased until cells could reach an infiltration rate of 99 μm at day 15 (Fig. 2P).

Altogether, these results showed that 3T3-L1 cells could attach, grow and colonize the whole tridimensional porous structure of the CAN during the 15 days of culture.

3.3. 3T3-L1 cells could produce lipid droplets when cultivated onto the CAN

We then investigated whether 3T3-L1 cells could differentiate into mature adipocytes when cultivated in CAN. The main characteristic of a

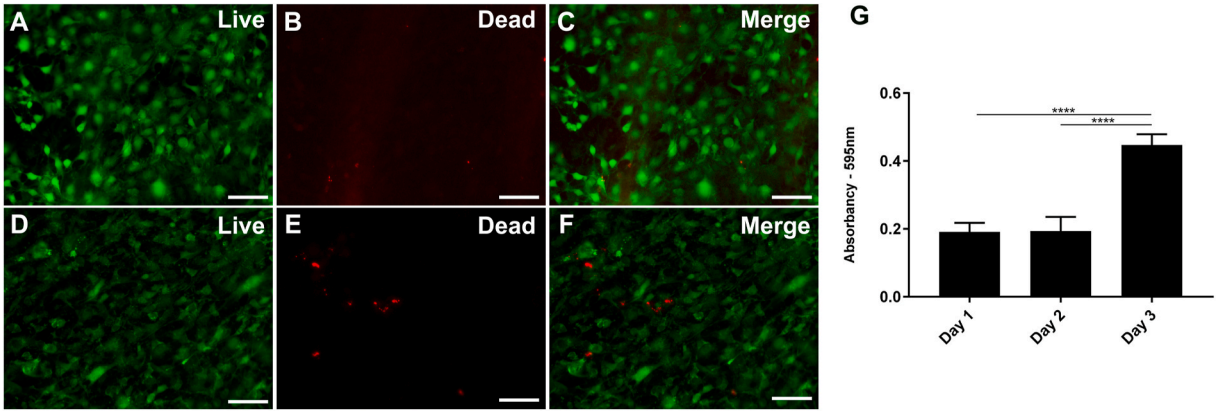

Fig. 1. Survival rate of 3T3-L1 cells on the CAN scaffold analyzed at 24 (A–C) and 72 h (D–F). Live/dead staining (green = live cells; red = dead cells). Scale bar: 100 μm. (G) - Cell viability through the MTT assay of 3T3-L1 cells on the CAN scaffold over 24h, 48h and 72 h. Mean ± SD ****p < 0.0001. (For interpretation of the references to color in this figure legend, the reader is referred to the Web version of this article.)

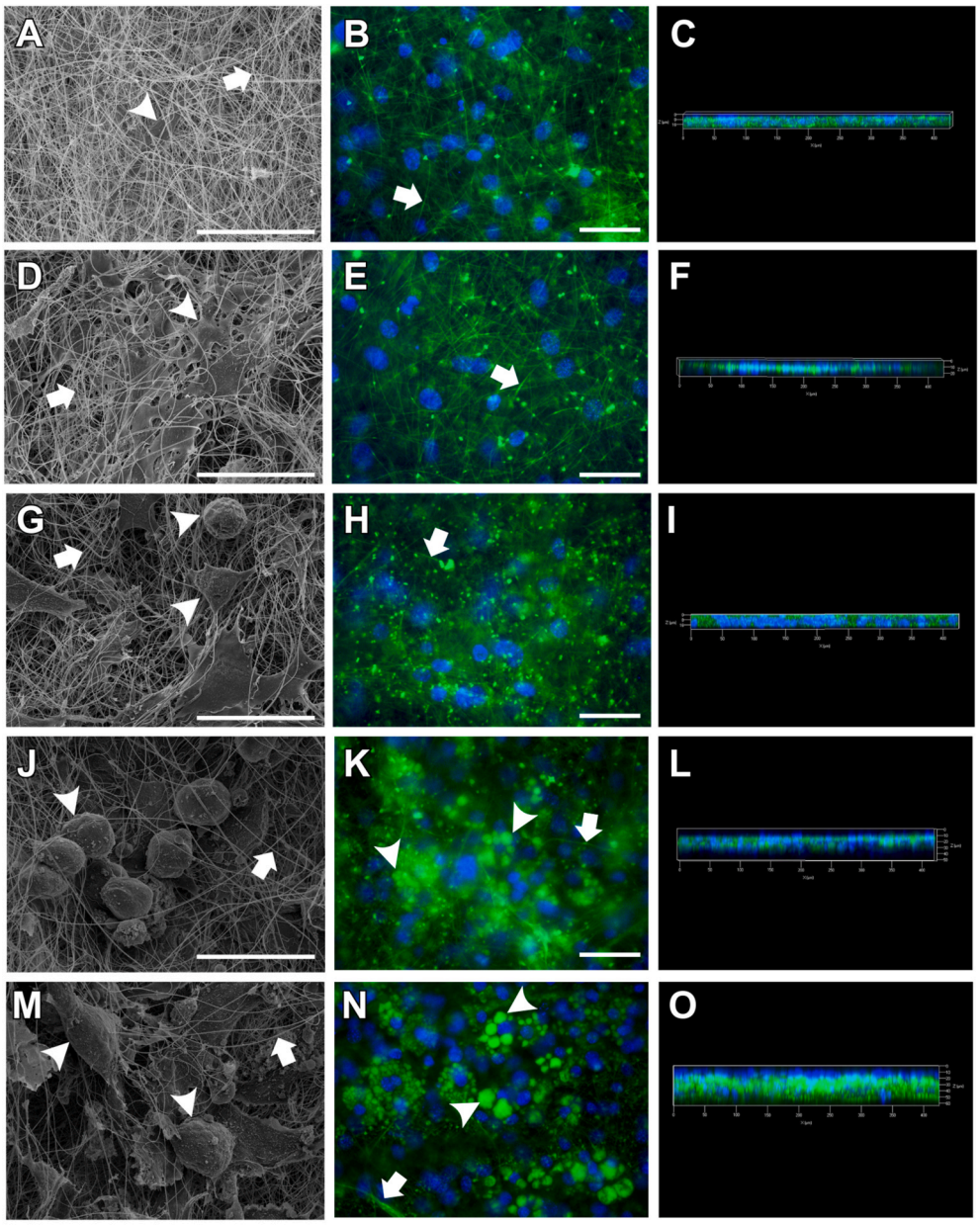

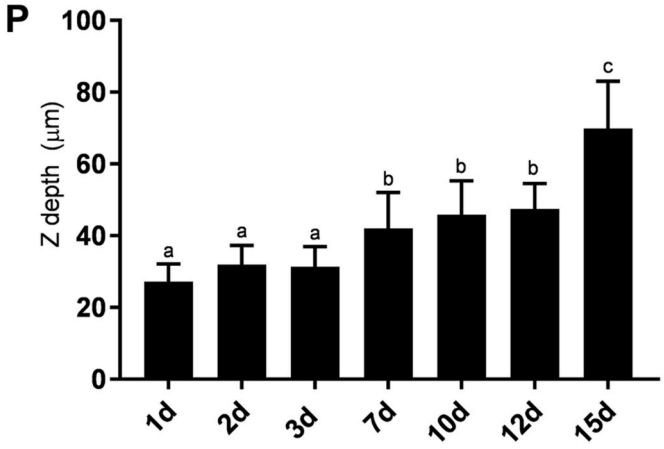

(caption on next page)

Fig. 2. Cell infiltration of 3T3-L1 cells growth on CAN scaffolds. SEM images after 1day (A), 3 days (D), 7 days (G), 10 days (J) and 15 days (M) of culture, CAN: arrow; cells: arrow head, scale bar: 50 μm. Bodipy Fluoresnce imagens showing nucleus (blue), CAN and lipid drops (both green) after 1day (B), 3 days (E), 7 days (H), 10 days (K) and 15 days (N) of culture, CAN: arrow; lipid drops: arrow head, scale bar: 50 μm. Confocal Z-stack images showing nucleus (blue), CAN and lipid drops (both green) after 1day (C), 3 days (F), 7 days (I), 10 days (L) and 15 days (O) of culture. Cell infiltration quantification on CAN, through analysis of the range of DAPI fluorescence of 1, 2, 3, 7, 10, 12 and 15 days of culture in the z-axis using confocal microscopy (P). Results are presented as mean ± SD, $p < 0.0001$. (For interpretation of the references to color in this figure legend, the reader is referred to the Web version of this article.)

differentiated adipocyte is its growing capacity to lipids in the form of droplets in their cytoplasm. These lipid droplets can be observed using different methods, here stained using both BODIPY and Oil red O.

A gradual increase of the number and size of lipid droplets in the cytoplasm of the cells could be observed throughout the differentiation induction (Fig. 3). Despite of the background caused by the staining of the CAN fibers with the BODIPY, the lipid droplets accumulation could be observed after 7 (Figs. 3A), 10 (Fig. 3B) and 12 days (Fig. 3C) of culture, becoming more evident after 15 days of culture, with cells presenting several large lipid droplets in their cytoplasm (Fig. 3D, arrows). However, DAPI/nuclei staining have also revealed the presence of "undifferentiated" cells, containing no lipid droplets in their cytoplasm (Fig. 3D, arrowhead), even after adipogenic differentiation induction and culture for 15 days.

Since the BODIPY could stain the fibers of the CAN, we decided to evaluate the capacity of these cells to differentiate also using Oil red O (Fig. 4). For this method, besides de cells cultivated onto the CAN, we decided to include a group of the cells cultivated as monolayer as a control group.

In the monolayer (Fig. 4A–E), a gradual increase of the number of cells containing lipid droplets could be observed from 4 (Fig. 4A) up to 10 days of culture (Fig. 4C). After 12 days of culture (Fig. 4D), however, cells began to detach from the bottom of the plate, living empty spaces (Fig. 4D and E) and reducing the amount of lipids that could be

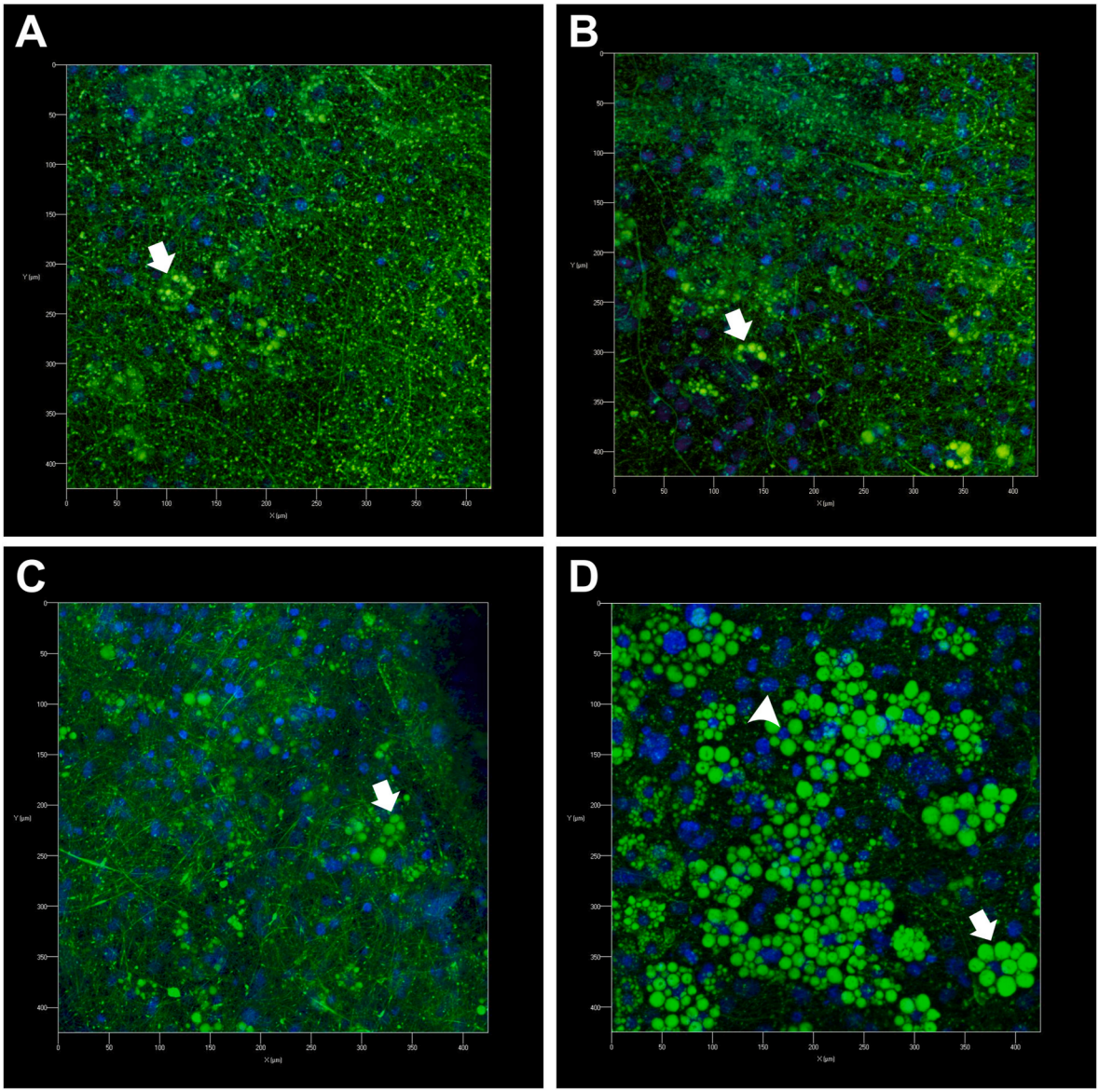

Fig. 3. Confocal images of 3T3-L1 adipogenic differentiation on CAN scaffold on 7 (A), 10 (B), 12 (C) and 15 days (D). Bodipy Fluoresnce imagens (green lipid drops and green nanofibers) with DAPI (blue nuclei) lipid drops: arrow; undifferentiated cell nucleus: arrowhead. (For interpretation of the references to color in this figure legend, the reader is referred to the Web version of this article.)

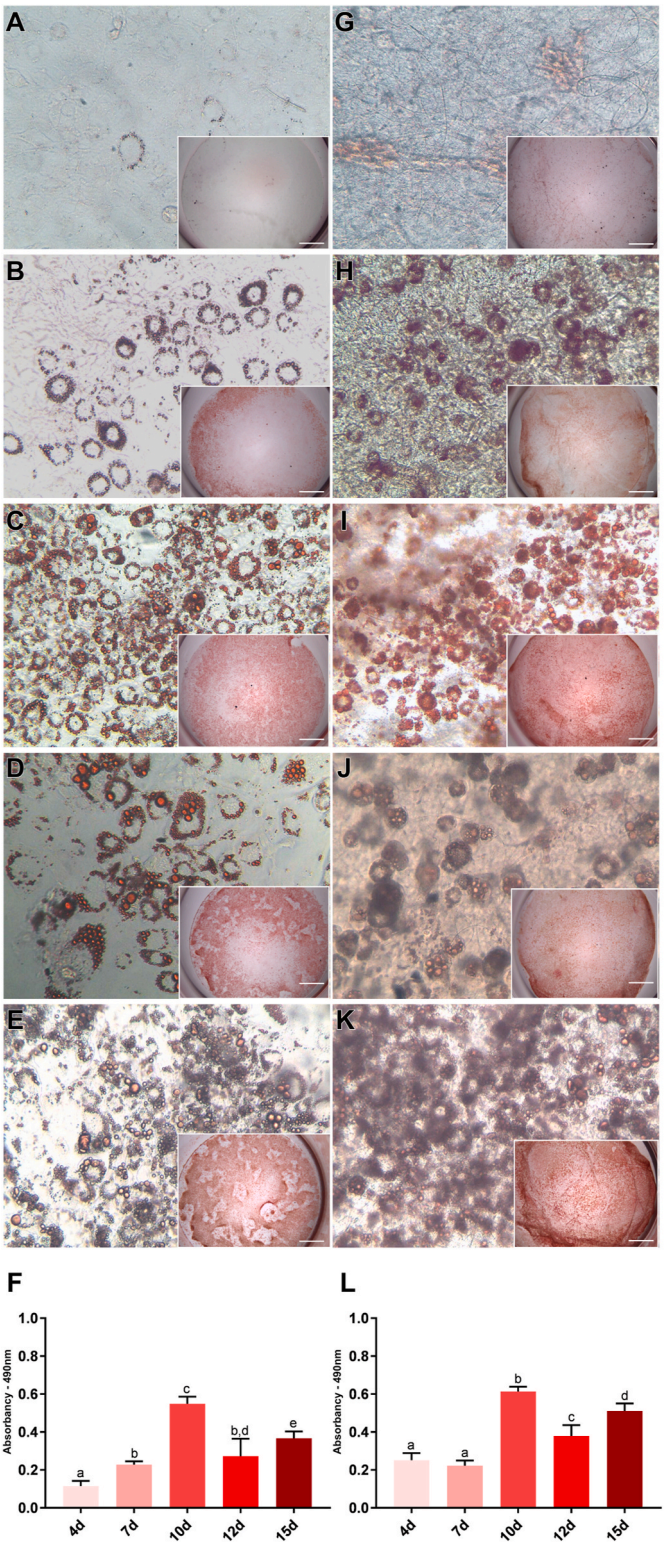

Fig. 4. – Adipogenic differentiation of 3T3-L1 in monolayer (A, B, C, D, E) and CAN scaffold (G, H, I, J, K) evaluated by Oil red O staining at different differentiation times - Day 4 (A, G), Day 7 (B, H), Day 10 (C, I), Day 12 (D, J), Day 15 (E, K). Inverted light microscope image (magnification 20×) and magnifying glass, scale bar: 2 mm. Percentage of lipid accumulation by quantification of Oil Red O in monolayer (F) and CAN scaffold (L) after 4, 7, 10, 12 and 15 days. Results are presented as mean ± SD, $p < 0.0001$. (For interpretation of the references to color in this figure legend, the reader is referred to the Web version of this article.)

quantified in the culture (Fig. 4F). When cells were seeded onto the scaffold (Fig. 4G–K), on the other hand, a gradual increase in the number and size of the droplets was also observed until the tenth day (Fig. 4I), followed by a decrease on day 12 (Fig. 4J). Nonetheless, unlike cells in monolayer culture, on day 15, we could observe a recovery in number of cells and in the quantity of lipid droplets stained with this method (Fig. 4K and L).

These results confirmed that the CAN did not interfere with 3T3-L1 fully differentiation into mature adipocytes and suggest that CAN avoided cell detachment in long-term culture.

3.4. SEM analysis revealed round-shaped cells

To obtain a more detailed information related to the cell shape upon differentiation onto CAN, we evaluated cell morphology using SEM.

As shown in Fig. 2, before the beginning of the differentiation process (2 days of culture), when cultivated only in GM, the cells exhibited the typical flat morphology, characteristic of undifferentiated mesenchymal cell (Fig. 5A). Similarly, on day 5 of culture, even after the differentiation induction, the cells still maintained their flat morphology (Fig. 5B). However, after two days in MM (7 days of culture), it was possible to observe some cells acquiring a more rounded shape (Fig. 5C, arrowheads). By the tenth day, the majority of the cells had acquired a rounded shape (Fig. 5D), and at the end of the differentiation process, 12 and 15 days of culture, most cells were firmly adhered to the scaffold surface and maintaining their spherical morphology (Fig. 5E and F).

Altogether, our results clearly show that 3T3-L1 cells reach fully differentiation when cultivated onto CAN and that the cells remain attached to CAN even after 15 days of culture.

3.5. 3T3-L1 expresses adipogenesis-related genes in CAN

To further determine the differentiation stage reached by these cells when cultivated onto CAN, qPCR was performed. For early differentiation stage, we quantified C/EBPβ and PPARγ transcripts, while Plin1 was used to quantify the presence of mature adipocytes. Gene expression analysis was performed only in cells cultivated onto CAN, along cell culture time (Fig. 6).

Our results showed no significative difference in the expression of C/EBPβ at 5 days (3 days in GM + 2 days in IM) compared with 3 days in culture (3 days in GM) (Fig. 6). After 10 and 15 days in culture, however, the expression of C/EBPβ was found to be downregulated (~0.052-fold change and ~0.094-fold change, respectively), compared to the expression detected after 3 days of culture (Fig. 6). PPARγ expression was upregulated after 5 days (~2.365-fold change) and 15 days (~1.929-fold change) of culture, both compared with the expression detected after 3 days in culture. No difference in the PPARγ expression was detected after 10 days, compared with 3 days (Fig. 6). Curiously, the expression of Plin1 marker was found to be significantly upregulated after 5 days (~315.537-fold change), 10 days (~361.621-fold change), and 15 days (~1280.75-fold change), all compared to 3 days of culture (Fig. 6).

Altogether, our results clearly show that 3T3-L1 cells activate genes related to the adipogenic cascade and that these cells can reach fully differentiation stage when cultivated onto the CAN.

3.6. Stackinng layers of CAN + differentiated cells and cooking

Finally, to form a cohesive and thicker tissue, we stacked four layers of CAN seeded with differentiated adipose cells over 15 days and investigated how the tissue would behave during the cooking process (Fig. 7).

Following the stacking, the tissue displayed a shiny appearance and a soft texture (Fig. 7A). After frying, we observed that the tissue acquired a crispy appearance and a brownish coloration (Fig. 7B).

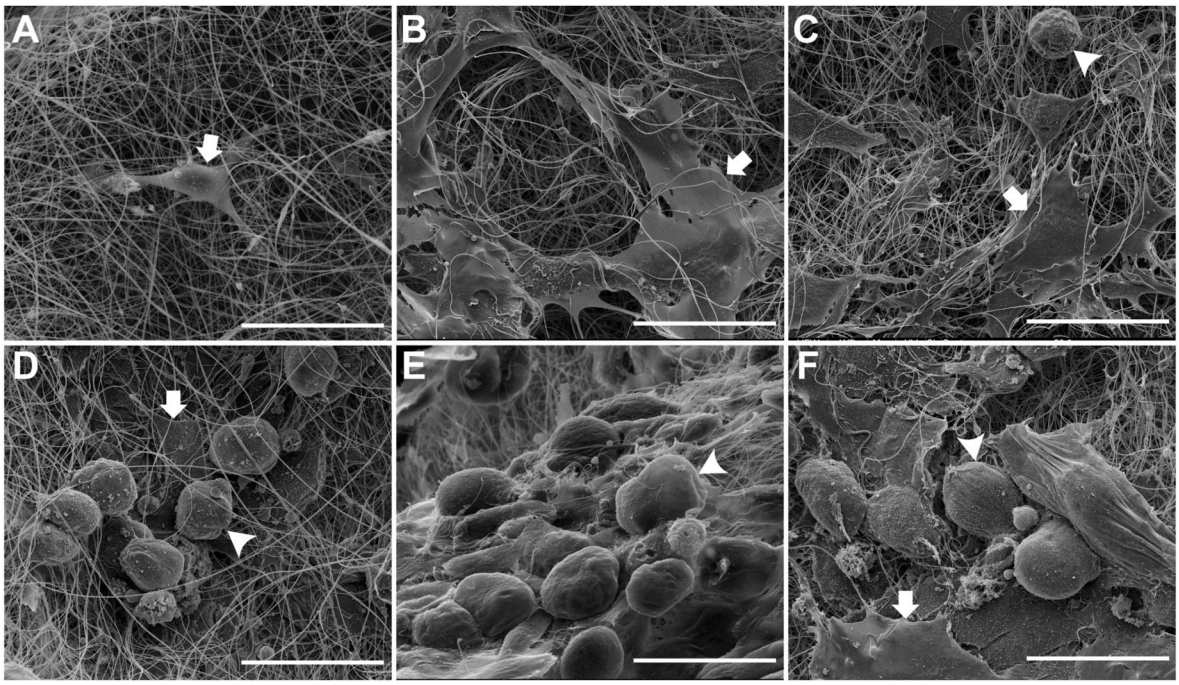

Fig. 5. SEM image of 3T3-L1 cells in CAN scaffold during adipogenic differentiation. Images of 1 (A), 5 (B), 7 (C), 10 (D), 12 (E) and 15 days (D). Arrows: flat cells, Arrows head: spherical cells. Scale bar: 50 μm.

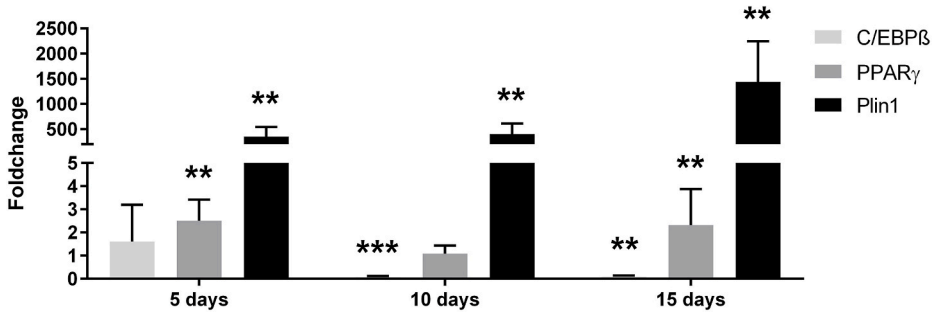

Fig. 6. – Expression levels of adipogenic-specific genes in 5, 10 and 15 days were compared to expression levels at 1 day in GM. Data is represented as mean ± SEM; **p < 0.01 and ***p < 0.001.

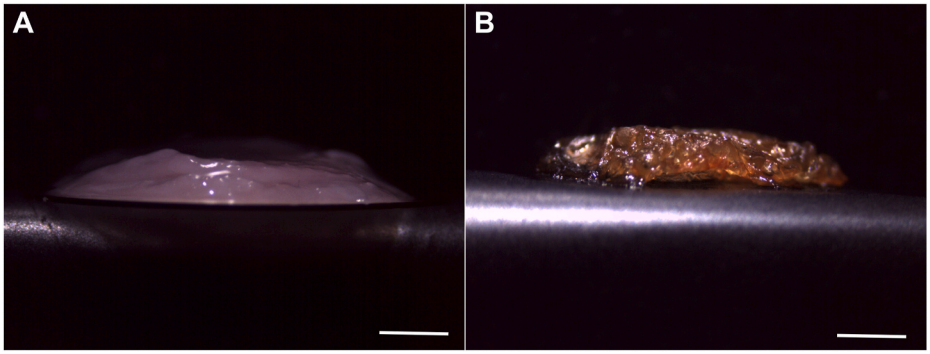

Fig. 7. Tissue development by stacking CAN scaffolds seeding with 3T3-L1 cells after 15 days of cultivation. (A) Macroscopic image of stacking. (B) Tissue fat fried. Scale bar: 2 mm.

4. Discussion

While most academic work on cell-cultured meat has focused on innovations for scalable muscle tissue culture, fat production is an important and often neglected component of this technology (Fish et al., 2020). Thus, to understand the capability of the fibrous scaffold produced by the electrospinning of cellulose acetate in forming structured adipose tissue, in this work we cultivated 3T3 pre-adipose cell line onto these cellulose acetate nanofibers and evaluated the capacity of these cells to attach, infiltrate, grow and differentiate into mature adipocytes.

The ability of preadipocytes to colonize in scaffolds is the primary condition for preparing cultured fat (Liu et al., 2023). Our results demonstrated that CAN did not induce significant cell death and promoted cell proliferation over the 72 h cultivation period. These findings are consistent with those previously observed in muscle cells. Prior studies (Santos et al., 2023a, 2023b) observed that immortalized myoblasts (C2C12 and H9C12) did not exhibit significant cell death during 72 h of cultivation, confirming this to be a biocompatible scaffold for cell culture, which can be used to expand cells before the differentiation process into muscle or adipose tissue.

In addition to being biocompatible and allowing cell attachment, another important premise for an ideal scaffold is its capacity for cell infiltration. Cellular behavior can be influenced by material properties, with high porosity being necessary for cells to infiltrate and migrate deep into the structure (Unnithan et al., 2018; Loh and Choong, 2013). Fibrous scaffolds have demonstrated such infiltration capacity; for example, pluripotent embryonic stem cells migrated on nanofibrous polycaprolactone scaffolds to a depth of 40 μm (Kang et al., 2007), while C2C12 myoblasts migrated 58 μm on cellulose acetate nanofiber (Santos et al., 2023b). In our results, this infiltration property was also observed from the first day of cultivation, progressively increasing until the last day, reaching a depth of 99 μm. Although the CAN has an approximate thickness of 100 μm (Santos et al., 2023b), the observed infiltration depth of 99 μm may have resulted from cell hypertrophy during the differentiation period (discussed further below). Adipocyte hypertrophy can reach an increase in size of several hundred micrometers in diameter (Horwitz and Birk, 2023). This expansion might have caused a displacement of adjacent cells, contributing to an overall increase in tissue volume and giving it a thicker appearance.

The goal of edible tissue engineering is to create tissue that will best mimic real fat tissue, i.e., lipid-rich adipose tissue. Understanding the natural process of adipogenesis might contribute to reach this objective (Zagury et al., 2022). Adipogenesis is the process by which mesenchymal stem cells (MSCs) differentiate into preadipocytes, which then further differentiate into mature adipocytes (Kim et al., 2020). During this process, lipid drop concentration increases in the cytoplasm and eventually coalesce gradually (Olzmann and Carvalho, 2019).

This process of differentiation of 3T3-L1 cells is described as easily visible, with intracellular lipid droplets appearing at around day 7 and increased in both number and size over the following days (Zebisch et al., 2012). We observed a similar pattern of differentiation of these cells when cultivated onto CAN, with a gradual increase in the lipid droplets from the 7th day that fuse over time, demonstrating that the scaffold did not interfere with the maturation of the adipocytes. This was also confirmed by the round shape observed for these cells in SEM analysis, characteristic of mature adipocytes.

Such ability of a fibrous scaffold to support adipogenic differentiation has been observed in other studies. Unithan et al. (Unnithan et al., 2018) demonstrated the adipogenic property of 3T3-L1 cells when cultivated on a zwitterionic poly co-polymer scaffold. Shanti et al. (2008) similarly observed the presence of lipid vesicles in human bone marrow-derived mesenchymal stem cells when cultured on a nanofibrous scaffold made of poly L-lactic acid. Scaffolds have proven to be essential structures for cultured fat production. One of the advantages is that these structures allow cell-cell and cell-matrix interactions to occur across the entire cell membrane surface, unlike a 2D surface, in which most of the cell membrane interacts with the stiff surface (Bomkamp et al., 2022).

Another advantage of scaffolds for cultivated fat production is the prevention of cell flotation. During the in vitro adipogenic differentiation, lipid droplet increases adipocyte buoyancy, making cell culture methods used for other cell types fairly ineffective as they rely on cells attaching to a culture plate whereas lipid-containing adipocytes float (Poulos et al., 2010). Therefore, three-dimensional biomaterials are even more required for these mature adipocytes than all the other cell types (Louis and Matsusaki, 2020), since these structures mimic the extracellular matrix (ECM), reconstructing the tissue architecture and providing structural support to adipocytes (Yoon and Park, 2023). This creates anchoring points and consequently prevents the cells from detaching.

We observed this aspect in our research. The cells seeded on CAN could differentiate and the scaffold prevented them to detach in the long-term culture, keeping them stuck into the scaffold during differentiation. In contrast, cells seeded directly on the plate formed non-uniform aggregates that detached during differentiation.

Other point to consider is that some of the cells did not differentiate even after 15 days in culture. Despite the majority of cells differentiating within 15 days, we observed a small population of cells that remained undifferentiated. This probably occurs due to the phenomenon known as mitotic clonal expansion, in which pre-adipocytes, when induced, undergo multiple rounds of mitosis before differentiating into adipocytes (Tang and Lane, 2012). This process can be attributed to the medium, rich in mitogens, which induces the entire population of cells to reenter the cell cycle (G0 to G1) and undergo at least two rounds of cell division before proceeding into terminal adipogenesis (Farmer, 2006).

Adipogenesis is controlled by a tightly regulated transcriptional cascade where the transcription factors activate or repress the expression of each other in a sequential manner (Siersbæk et al., 2012). Once committed, preadipocytes progressively acquire an adipocyte-specific gene expression pattern along with lipid droplet formation (Dufau et al., 2021). This process is regulated at the molecular level by several key transcription factors, including peroxisome proliferator-activated receptor gamma (PPARγ) and CCAAT/enhancer-binding proteins (C/EBPs) (Pu et al., 2017; Cahyadi et al., 2023). These factors subsequently lead to the expression of genes characteristic of mature adipocytes, such as Plin1, FABP4, and Adipoq (Song et al., 2022b).

Adipogenesis-inducing agents - Insulin, dexamethasone, 3-isobutyl-1-methylxanthine (IBMX) and indomethacin - are used to induce preadipocyte differentiation, enhancing master early regulators of adipocyte differentiation and subsequent lipid accumulation (Sugii et al., 2023; Farmer, 2006; Shang et al., 2014). C/EBP-β and -δ are the first transcription factors induced after cells are exposed to adipogenesis-inducing agents (César Farias de et al., 2009). These genes induce low levels of PPARγ and C/EBP-α, which are then able to induce each other's expression in a positive feedback loop that promotes and maintains the differentiated state (Rosen et al., 2002). This, in turn, coordinately activates genes whose expression produces the adipocyte phenotype (Tang and Lane, 2012). C/EBP-β is activated by dexamethasone, a synthetic glucocorticoid, and IBMX, a phosphodiesterase inhibitor that increases intracellular cAMP (Mitić et al., 2023), but not by insulin, which directly modulates the expression of PPARγ (Chen et al., 2013). This statement aligns with our results, which showed that C/EBP-β was found to be downregulated at 10 and 15 days when only insulin was present in the medium (maintenance medium - DMEM supplemented with FBS and insulin), without the presence of dexamethasone and IBMX. Additionally, we found PPARγ to be upregulated at 5 and 15 days. PPARγ is one of the most important early transcription factors, indirectly triggered by dexamethasone, IBMX, indomethacin, and directly triggered by insulin (Berry et al., 2016; Overby et al., 2020). Therefore, its activation is expected in both induction (DMEM supplemented with FBS, insulin, dexamethasone, IBMX and indomethacin) and maintenance media (DMEM supplemented with FBS and insulin). However, the expression of PPARγ at 10 days was not significant. This may have occurred because PPARγ and C/EBPα self-regulate (César Farias de et al., 2009). Thus, during this self-regulation process, when one of these genes is highly expressed, the other may be low. Therefore, it is probable that C/EBPα was being expressed at 10 days.

Induction of differentiation triggers deep phenotypic changes in preadipocytes as they transition to mature adipocytes (Cahyadi et al., 2023). Such phenotypic changes occur due to late-expressed genes, such as Plin1. Plin1 is one of the most abundant proteins in lipid droplet surfaces which plays a vital role during fat metabolism of adipose tissue

lipolysis and fat storage in adipocytes (Li et al., 2020). We observed that the levels of Plin1 were highly expressed from day 5, indicating that, from the beginning of induction - even in cells still in a flat shape, characteristic of undifferentiated cells and with few lipid droplets in the cytoplasm - the differentiation cascade was activated and the cells were already differentiating, showing this protocol to be effective.

Finally, aiming to establish a cohesive structure at a tissue scale, we stacked layers of CAN with mature adipocytes. The appearance and texture of the constructed tissue resembles natural adipose tissue, with a shiny appearance and soft texture. Furthermore, after cooking, the tissue acquired a crispy appearance and brownish coloration characteristics of conventional meat products. Thus, aggregating smaller adipose tissue constructs that are separately cultivated may be an alternative strategy to forming macroscale adipose tissue, which could circumvent the need for nutrient perfusion and being an approach for mimicking the natural structure and texture of meat (Yuen et al., 2022; Li et al., 2022).

5. Conclusion

In this study, we evaluated the effectiveness of cellulose acetate nanofiber scaffolds (CAN) for cultivating adipose tissue. For this, we seeded cells of the 3T3-L1 lineage on the scaffold and induced differentiation, then, evaluated biocompatibility, adhesion, efficiency, and lipid production. Our results showed that CAN was able to prevent cell fluctuation, maintaining cell regularity and differentiation. Even though primary cells from animals of economic interest are not used here, the 3T3-L1 lineage is a valuable research tool that can be used to deepen the understanding of cellular characteristics relevant to the biomanufacturing of adipose tissue (Fish et al., 2020), requiring further testing the use of primary cells on this scaffold to evaluate their behavior on the scaffold and their differentiation process. Furthermore, it is important to consider the adipogenesis-inducing agents, which, although efficient for differentiation, are unsuitable for consumption. Therefore, it is necessary to investigate compounds that are safe for consumption, exploring alternative methods to induce differentiation.

CRediT authorship contribution statement

Amanda Maria Siqueira Moreira: Conceptualization, Formal analysis, Investigation, Methodology, Visualization, Writing – original draft. **Júlia Meireles Nogueira:** Formal analysis, Investigation, Methodology. **Jade Carceroni:** Formal analysis, Investigation, Methodology. **Jorge Luís Guadalupe:** Formal analysis, Investigation, Methodology. **Ana Elisa Antunes dos Santos:** Formal analysis, Investigation, Methodology. **Ana Maria Alvarenga Fagundes:** Formal analysis, Investigation, Methodology. **Aline Gonçalves Lio Copola:** Formal analysis, Investigation, Methodology. **Gerluza Aparecida Borges Silva:** Methodology. **Aline Bruna da Silva:** Methodology. **João Paulo Ferreira Santos:** Methodology. **Juliano Douglas Silva Albergaria:** Formal analysis, Investigation, Methodology. **Luciana de Oliveira Andrade:** Conceptualization, Resources, Writing – review & editing. **Erika Cristina Jorge:** Conceptualization, Resources, Writing – review & editing, Funding acquisition, Project administration, Supervision, All authors listed have made a substantial, direct and intellectual contribution to the worked and approved it for publication.

Funding

This study was conducted with the support of The Good Food Institute (GFI), through the 2021 GFI Competitive Grant Program.

Declaration of competing interest

The authors declare that they have no known competing financial interests or personal relationships that could have appeared to influence the work reported in this paper.

Acknowledgements

The authors are grateful to Centro de Aquisição e Processamento de Imagens (CAPI/ICB), Centro de Microscopia da UFMG, Centro de Desenvolvimento da Tecnologia Nuclear da UFMG and Laboratório Idea Real (ICB/UFMG).

Appendix A. Supplementary data

Supplementary data to this article can be found online at https://doi.org/10.1016/j.crfs.2024.100903.

Data availability

Data will be made available on request.

References

Berry, R., Fretz, J.A., MacDougald, O., Klibansky, A., Rosen, C.J., Rodeheffer, M.S., et al., 2016. Marrow adipose tissue and its interactions with the skeletal, hematopoietic, and immune systems. Osteoimmunology: Interactions of the Immune and Skeletal Systems, second ed. Elsevier Inc., pp. 345–352. https://doi.org/10.1016/B978-0-12-800571-2.00020-7

Bomkamp, C., Skaalure, S.C., Fernando, G.F., Ben-Arye, T., Swartz, E.W., Specht, E.A., 2022. Scaffolding biomaterials for 3D cultivated meat: prospects and challenges. Adv. Sci. 9. https://doi.org/10.1002/advs.202102908.

Cahyadi, D.D., Warita, T., Irie, N., Mizoguchi, K., Tashiro, J., Hosaka, Y.Z., et al., 2023. Housekeeping gene expression variability in differentiating and non-differentiating 3T3-L1 cells. Adipocyte 12. https://doi.org/10.1080/21623945.2023.2235081.

Cawthorn, W.P., Scheller, E.L., MacDougald, O.A., 2012. Adipose tissue stem cells meet preadipocyte commitment: going back to the future. J. Lipid Res. 53, 227–246. https://doi.org/10.1194/jlr.R021089.

César Farias de Queiroz, J., Isabel Cardoso Alonso-Vale, M., Curi, R., Bessa Lima, F., 2009. Controle da adipogênese por ácidos graxos Control of adipogenesis by fatty acids, vol. 53.

Chen, L., Li, Q.Y., Shi, X.J., Mao, S.L., Du, Y.L., 2013. 6-Hydroxydaidzein enhances adipocyte differentiation and glucose uptake in 3T3-L1 cells. J. Agric. Food Chem. 61, 10714–10719. https://doi.org/10.1021/jf402694m.

Dohmen, R.G.J., Hubalek, S., Melke, J., Messmer, T., Cantoni, F., Mei, A., et al., 2022. Muscle-derived fibro-adipogenic progenitor cells for production of cultured bovine adipose tissue. NPJ Sci Food 6. https://doi.org/10.1038/s41538-021-00122-2.

dos Santos, A.E.A., dos Santos, F.V., Freitas, K.M., Pimenta, L.P.S., de Oliveira Andrade, L., Marinho, T.A., et al., 2021. Cellulose acetate nanofibers loaded with crude annatto extract: preparation, characterization, and in vivo evaluation for potential wound healing applications. Mater. Sci. Eng. C 118. https://doi.org/10.1016/j.msec.2020.111322.

Dufau, J emy, Shen, J.X., Couchet, M., de Castro Barbosa, T., Mejhert, N., Massier, L., et al., 2021. In vitro and ex vivo models of adipocytes. Am J Physiol Cell Physiol 320, C822–C841. https://doi.org/10.1152/ajpcell.00519.2020.

Farmer, S.R., 2006. Transcriptional control of adipocyte formation. Cell Metab 4, 263–273. https://doi.org/10.1016/j.cmet.2006.07.001.

Fish, K.D., Rubio, N.R., Stout, A.J., Yuen, J.S.K., Kaplan, D.L., 2020. Prospects and challenges for cell-cultured fat as a novel food ingredient. Trends Food Sci. Technol. 98, 53–67. https://doi.org/10.1016/j.tifs.2020.02.005.

Hocquette, J.F., Gondret, F., Baza, E., Mdale, F., Jurie, C., Pethick, D.W., 2010. Intramuscular fat content in meat-producing animals: development, genetic and nutritional control, and identification of putative markers. Animal 4, 303–319. https://doi.org/10.1017/S1751731109991091.

Horwitz, A., Birk, R., 2023. Adipose tissue hyperplasia and hypertrophy in common and syndromic obesity—the case of BBS obesity. Nutrients 15. https://doi.org/10.3390/nu15153445.

Kang, X., Xie, Y., Powell, H.M., James Lee, L., Belury, M.A., Lannutti, J.J., et al., 2007. Adipogenesis of murine embryonic stem cells in a three-dimensional culture system using electrospun polymer scaffolds. Biomaterials 28, 450–458. https://doi.org/10.1016/j.biomaterials.2006.08.052.

Kim, D.H., Lee, J., Suh, Y., Cressman, M., Lee, K., 2020. Research Note: all-trans retinoic acids induce adipogenic differentiation of chicken embryonic fibroblasts and preadipocytes. Poult Sci 99, 7142–7146. https://doi.org/10.1016/j.psj.2020.09.006.

Kumar, P., Sharma, N., Sharma, S., Mehta, N., Verma, A.K., Chemmalar, S., et al., 2021. In-vitro meat: a promising solution for sustainability of meat sector. J. Anim. Sci. Technol. 63, 693–724. https://doi.org/10.5187/jast.2021.e85.

Levi, S., Yen, F.C., Baruch, L., Machluf, M., 2022. Scaffolding technologies for the engineering of cultured meat: towards a safe, sustainable, and scalable production. Trends Food Sci. Technol. 126, 13–25. https://doi.org/10.1016/j.tifs.2022.05.011.

Li, S., Raza, S.H.A., Zhao, C., Cheng, G., Zan, L., 2020. Overexpression of PLIN1 promotes lipid metabolism in bovine adipocytes. Animals 10, 1–14. https://doi.org/10.3390/ani10111944.

Li, C.H., Yang, I.H., Ke, C.J., Chi, C.Y., Matahum, J., Kuan, C.Y., et al., 2022. The production of fat-containing cultured meat by stacking aligned muscle layers and adipose layers formed from gelatin-soymilk scaffold. Front. Bioeng. Biotechnol. 10. https://doi.org/10.3389/fbioe.2022.875069.

Liu, P., Song, W., Bassey, A.P., Tang, C., Li, H., Ding, S., et al., 2023. Preparation and quality evaluation of cultured fat. J. Agric. Food Chem. 71, 4113–4122. https://doi.org/10.1021/acs.jafc.2c08004.

Loh, Q.L., Choong, C., 2013. Three-dimensional scaffolds for tissue engineering applications: role of porosity and pore size. Tissue Eng Part B Rev 19, 485–502. https://doi.org/10.1089/ten.teb.2012.0437.

Louis, F., Matsusaki, M., 2020. Adipose tissue engineering. Biomaterials for Organ and Tissue Regeneration: New Technologies and Future Prospects. Elsevier, pp. 393–423. https://doi.org/10.1016/B978-0-08-102906-0.00008-8.

Mitić, R., Cantoni, F., Börlin, C.S., Post, M.J., Jackisch, L., 2023. A simplified and defined serum-free medium for cultivating fat across species. iScience 26. https://doi.org/10.1016/j.isci.2022.105822.

Olzmann, J.A., Carvalho, P., 2019. Dynamics and functions of lipid droplets. Nat. Rev. Mol. Cell Biol. 20, 137–155. https://doi.org/10.1038/s41580-018-0085-z.

Overby, H., Yang, Y., Xu, X., Wang, S., Zhao, L., 2020. Indomethacin promotes browning and brown adipogenesis in both murine and human fat cells. Pharmacol Res Perspect 8. https://doi.org/10.1002/prp2.592.

Pfaffl, M.W., Horgan, G.W., Dempfle, L., 2002. Relative Expression Software Tool (REST©) for Group-wise Comparison and Statistical Analysis of Relative Expression Results in Real-Time PCR, vol. 30.

Poulos, S.P., Dodson, M.V., Hausman, G.J., 2010. Cell line models for differentiation: preadipocytes and adipocytes. Exp Biol Med 235, 1185–1193. https://doi.org/10.1258/ebm.2010.010063.

Pu, Y., Veiga-Lopez, A., 2017. PPARγ agonist through the terminal differentiation phase is essential for adipogenic differentiation of fetal ovine preadipocytes. Cell. Mol. Biol. Lett. 22. https://doi.org/10.1186/s11658-017-0037-1.

Rosen, E.D., Hsu, C.H., Wang, X., Sakai, S., Freeman, M.W., Gonzalez, F.J., et al., 2002. C/EBPα induces adipogenesis through PPARγ: a unified pathway. Genes Dev. 16, 22–26. https://doi.org/10.1101/gad.948702.

Rubio, N.R., Xiang, N., Kaplan, D.L., 2020. Plant-based and cell-based approaches to meat production. Nat. Commun. 11. https://doi.org/10.1038/s41467-020-20061-y.

Santos, A.E.A. dos, Cotta, T., Santos, J.P.F., Camargos, J.S.F., Carmo, ACC do, Alcântara, E.G.A., et al., 2023a. Bioactive cellulose acetate nanofiber loaded with annatto support skeletal muscle cell attachment and proliferation. Front. Bioeng. Biotechnol. 11. https://doi.org/10.3389/fbioe.2023.1116917.

dos Santos, A.E.A., Guadalupe, J.L., Albergaria, J.D.S., Almeida, I.A., Moreira, A.M.S., Copola, A.G.L., et al., 2023b. Random cellulose acetate nanofibers: a breakthrough for cultivated meat production. Front. Nutr. 10. https://doi.org/10.3389/fnut.2023.1297926.

Seah, J.S.H., Singh, S., Tan, L.P., Choudhury, D., 2022. Scaffolds for the manufacture of cultured meat. Crit. Rev. Biotechnol. 42, 311–323. https://doi.org/10.1080/07388551.2021.1931803.

Shang, Z., Guo, L., Wang, N., Shi, H., Wang, Y., Li, H., 2014. Oleate promotes differentiation of chicken primary preadipocytes in vitro. Biosci. Rep. 34, 51–57. https://doi.org/10.1042/BSR20130120.

Shanti, R.M., Janjanin, S., Li, W.J., Nesti, L.J., Mueller, M.B., Tzeng, M.B., et al., 2008. In vitro adipose tissue engineering using an electrospun nanofibrous scaffold. Ann. Plast. Surg. 61, 566–571. https://doi.org/10.1097/SAP.0b013e31816d9579.

Siersbæk, R., Nielsen, R., Mandrup, S., 2012. Transcriptional networks and chromatin remodeling controlling adipogenesis. Trends Endocrinol. Metabol. 23, 56–64. https://doi.org/10.1016/j.tem.2011.10.001.

Song, W.J., Liu, P.P., Zheng, Y.Y., Meng, Z.Q., Zhu, H.Z., Tang, C.B., et al., 2022a. Production of cultured fat with peanut wire-drawing protein scaffold and quality evaluation based on texture and volatile compounds analysis. Food Res. Int. 160. https://doi.org/10.1016/j.foodres.2022.111636.

Song, W.J., Liu, P.P., Meng, Z.Q., Zheng, Y.Y., Zhou, G.H., Li, H.X., et al., 2022b. Identification of porcine adipose progenitor cells by fluorescence-activated cell sorting for the preparation of cultured fat by 3D bioprinting. Food Res. Int. 162. https://doi.org/10.1016/j.foodres.2022.111952.

Su, L., Jing, L., Zeng, S., Fu, C., Huang, D., 2024. 3D porous edible scaffolds from rye secalin for cell-based pork fat tissue culturing. J. Agric. Food Chem. 72, 11587–11596. https://doi.org/10.1021/acs.jafc.3c09713.

Sugii, S., Wong, C.Y.Q., Lwin, A.K.O., Chew, L.J.M., 2023. Alternative fat: redefining adipocytes for biomanufacturing cultivated meat. Trends Biotechnol. 41, 686–700. https://doi.org/10.1016/j.tibtech.2022.08.005.

Tang, Q.Q., Lane, M.D., 2012. Adipogenesis: from stem cell to adipocyte. Annu. Rev. Biochem. 81, 715–736. https://doi.org/10.1146/annurev-biochem-052110-115718.

Unnithan, A.R., Sasikala, A.R.K., Thomas, S.S., Nejad, A.G., Cha, Y.S., Park, C.H., et al., 2018. Strategic design and fabrication of biomimetic 3D scaffolds: unique architectures of extracellular matrices for enhanced adipogenesis and soft tissue reconstruction. Sci. Rep. 8. https://doi.org/10.1038/s41598-018-23966-3.

Yoon, H., Park, T.-E., 2023. Engineered adipose tissue platforms: recent breakthroughs and future perspectives. Organoid 3, e1. https://doi.org/10.51335/organoid.2023.3.e1.

Yuen, J.S.K., Stout, A.J., Kawecki, N.S., Letcher, S.M., Theodossiou, S.K., Cohen, J.M., et al., 2022. Perspectives on scaling production of adipose tissue for food applications. Biomaterials 280. https://doi.org/10.1016/j.biomaterials.2021.121273.

Zagury, Y., Ianovici, I., Landau, S., Lavon, N., Levenberg, S., 2022. Engineered marble-like bovine fat tissue for cultured meat. Commun. Biol. 5. https://doi.org/10.1038/s42003-022-03852-5.

Zebisch, K., Voigt, V., Wabitsch, M., Brandsch, M., 2012. Protocol for effective differentiation of 3T3-L1 cells to adipocytes. Anal. Biochem. 425, 88–90. https://doi.org/10.1016/j.ab.2012.03.005.